The measurements of the gamma-ray emission cross sections and angular distributions from (n,Xγ) reactions with 14.1 MeV neutrons with O, Al, Si, Ti, and Fe nuclei.

Grozdanov D.N., *Fedorov N.A., Prusachenko P.S., Kopach Yu.N., Hramko C., Ruskov I.N., Filonchk P.G., Kharlamov P.I., Tretyakova T.Yu., Skoi V.R., Zuev A.P., Andreev A.V., Pampushik G.V. and Tangra collaboration*

The work was carried out with the financial support of the RSCF (grant No. 23-12-00239).

Applications of fast neutrons

Elemental analysis in industry

Search for dangerous substances

Logging of oil, gas and ore deposits

Elemental analysis of soils

Design of nuclear power plants

The specified values of the cross sections are required

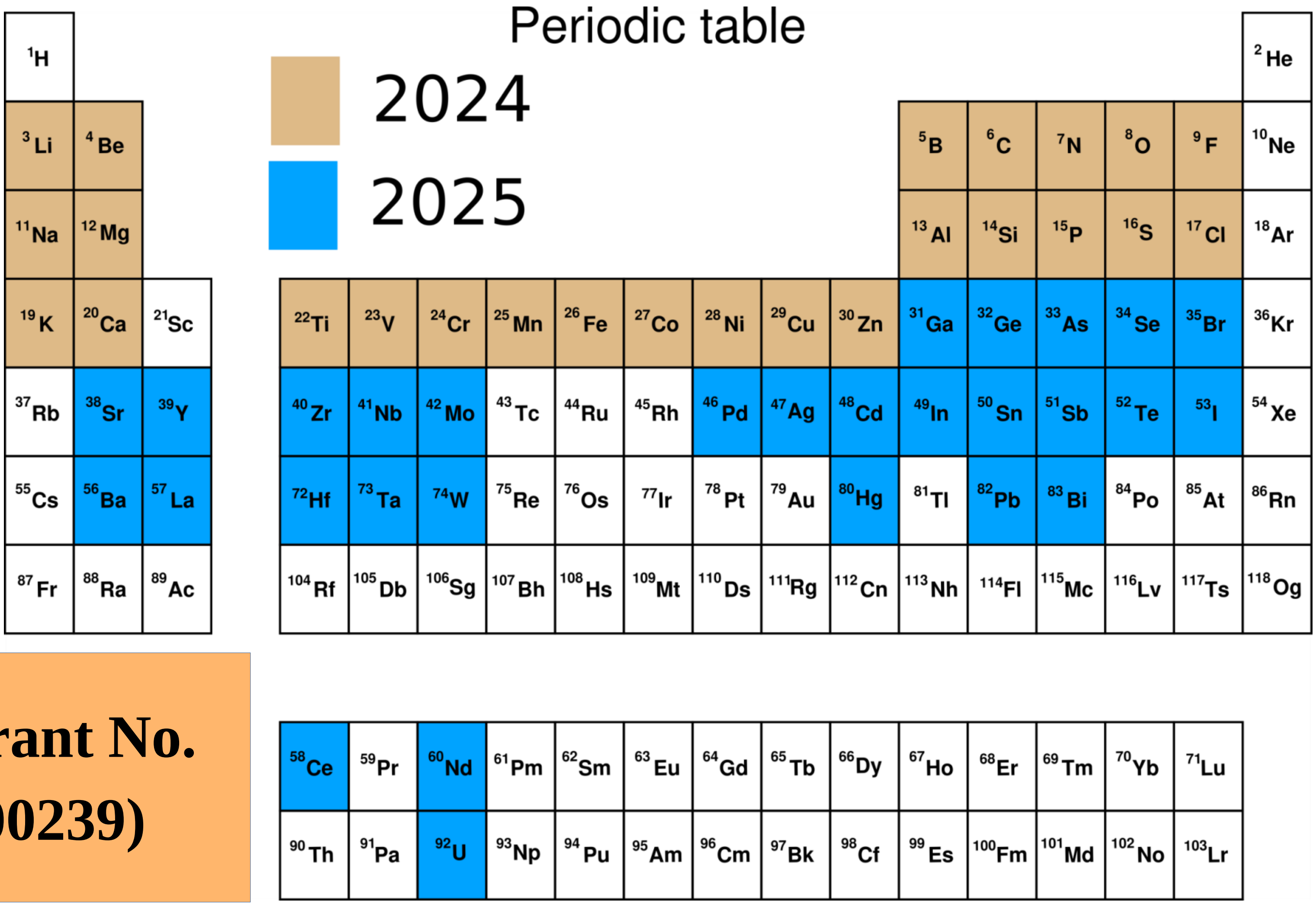

RSCF (grant No. 23-12-00239)

Cross-section data sources

4439	$^{12}C(n,n')^{12}C$	$4439(2^+)\to0(0^+)$, p

15.4	188±18
14.9	179±20
14.1	165±7
14.9	185±11
14.9	155±25
14.2	217±30
14.2	145±28
14	237±26
14.2	157±20
14.2	208±29
14.8	174±21
13.0	(s) 384±80
14.8	236±30
14.1	115±21
14.2	152±30
14.7	184±18
14	115±17
14.1	217±18
=14	230±28

The discrepancy is two times!!!

4439	$^{12}C(n,n')^{12}C$	$4439(2^+)\to0(0^+)$, p	15.4	90	Ø190×Ø110×??, +/+	Ge(Li)	170±20	Lashuk	1994	0.85	1.07	+33.3	188±18
			14.9	90	C:Ø28.0×35.4, 43g, +/+	Ge(Li)	153±19	Hongyu	1989	1.0	1.07	+15.0	179±20
			14.1	30-150	Ø30×Ø26×70, +/+	Ge	180±7	Murata	1988	?	1.0	-14.8	165±7
			14.9	90	C:Ø30×30, +/+	Ge(Li)	159±10	Hongyu	1986	1.0	1.07	+15.0	185±11
			14.9	93	No Information	NaI(Tl)	131±23	Zong-Ren	1979	1.0	1.07	+15.0	155±25
			14.2	45-130	Ø44×6,Ø31×Ø25×32,+/+	NaI(Tl)	228±30	Drake	1978	1.0	1.0	-11.1	217±30
			14.2	55	C:Ø30×40, +/+	Ge(Li)	156±28	Hino	1976	1.0	1.0	-11.1	145±28
			14	0-180	Ø60×Ø20, +/-	NaI(Tl)	255±26	Bezotosny	1976	1.0	1.0	-18.5	237±26
			14.2	125	C:Ø483×Ø279×25, +/+	Ge(Li)	168±20	Rogers	1975	1.0	1.0	-11.1	157±20
			14.2	45-125	No Information, +/+	NaI(Tl)	219±29	Arthur	1975	1.0	1.0	-11.1	208±29
			14.8	90	No Information	Ge(Li)	152±20	Martin	1971	1.0	1.07	+11.1	174±21
			13.0	30-140	C:Ø25.4×50.8, +/+	Antico	440±80	Morgan	1971	1.0	1.0	-55.5	(s) 384±80
			14.8	30-140	C:Ø25.4×50.8, +/+	Antico	225±30	Morgan	1971	1.0	1.0	+11.1	236±30
			14.1	90	C:Ø50×30, +/+	Ge(Li)	121±20	Clayeux	1969	1.0	1.07	-14.8	115±21
			14.2	0-180	Shell ??, +/+	NaIpair	163±30	Maslov	1968	1.0	1.0	-11.1	152±30
			14.7	90	C:Ø38.1×76.2, +/+	NaI(Tl)	165±17	Engesser	1967	1.0	1.07	+7.2	184±18
			14	No Inf	C:Ø60×30, +/+	NaI(Tl)	133±17	Bezotosny	1966	1.0	?	-18.5	115±17
			14.1	30-160	C:Ø??×20, +/+	NaI(Tl)	232±18	Stewart	1964	1.0	1.0	-14.8	217±18
			=14	30-150	C:Ø165×Ø115×25, +/+	NaI	249±28	Benveniste	1960	1.0	1.0	-18.5	230±28

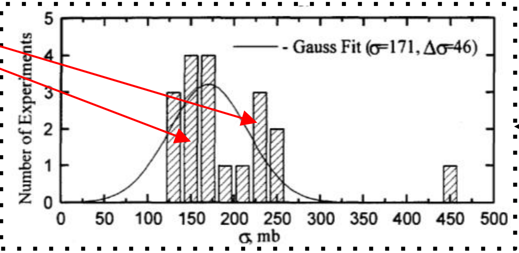

Distribution of experimental results by radiation cross sections of gamma quanta with an energy of 4439 keV in the reaction $^{12}C(n,n'\gamma)^{12}C^*$;

Nowadays, the most complete collection of data on reaction cross sections (n,n' γ) for neutrons with an energy of 14.5 MeV is presented in INDC(CCP)-413 (*Status of experimental and evaluated discrete γ-ray production at* E_n*=14.5 MeV*) 1998 г.

Cross-section data sources

https://doi.org/10.61092/iaea.y3q8-a4b5

INDC(NDS)-0740
Distr. ST, G

IAEA
International Atomic Energy Agency

INDC International Nuclear Data Committee

Evaluation of the ^{48}Ti(n,n′γ_{984keV}) γ-ray production cross section for standards

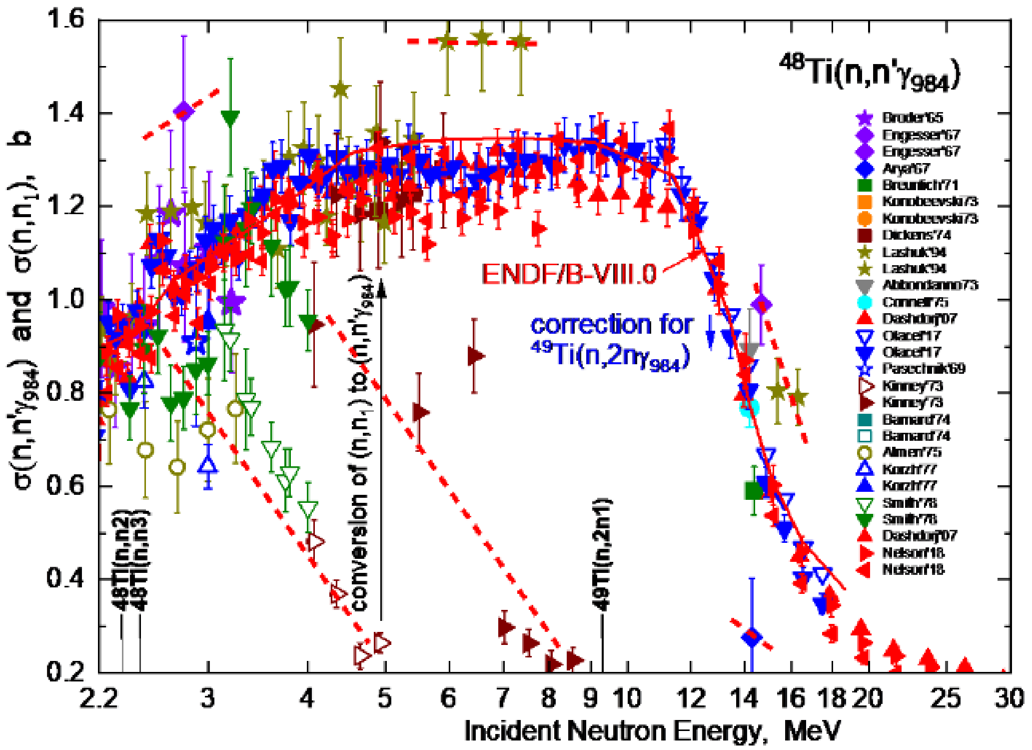

Tagged neutron method

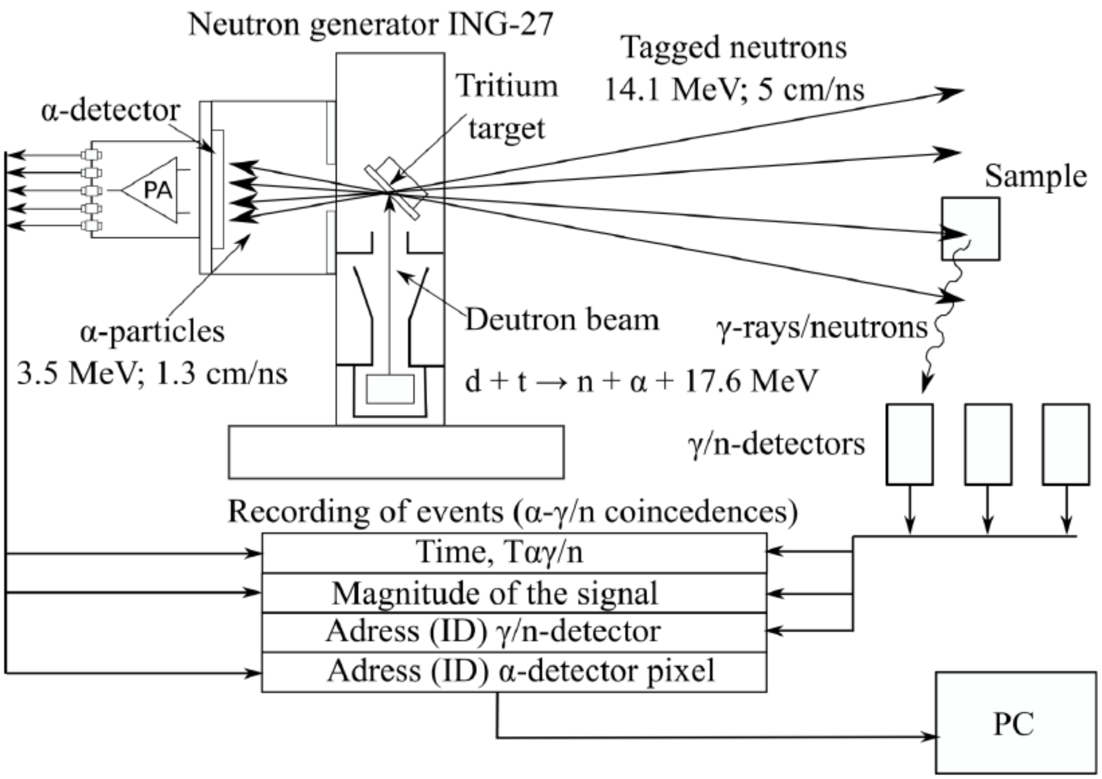

Experimental setup

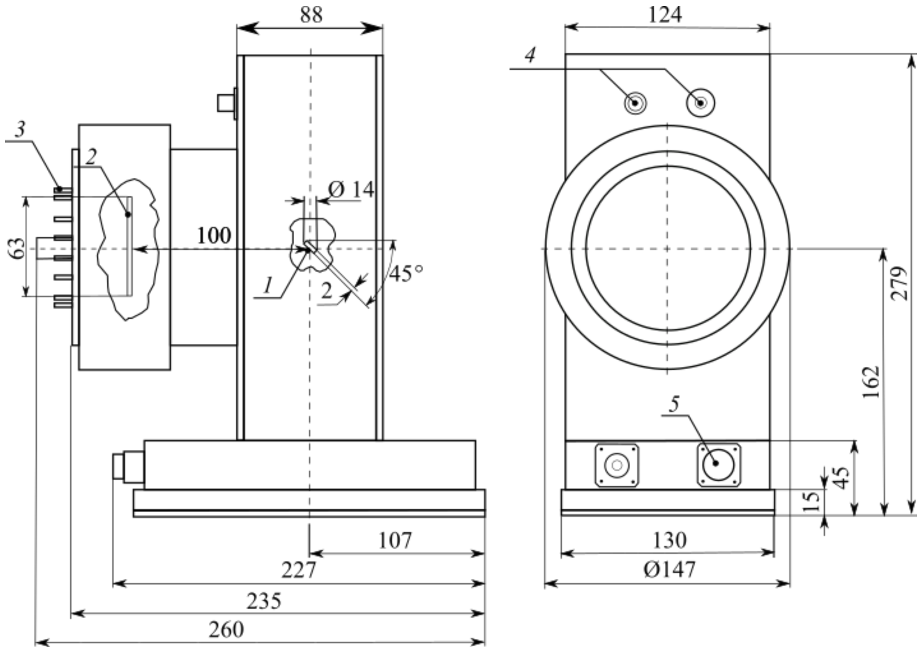

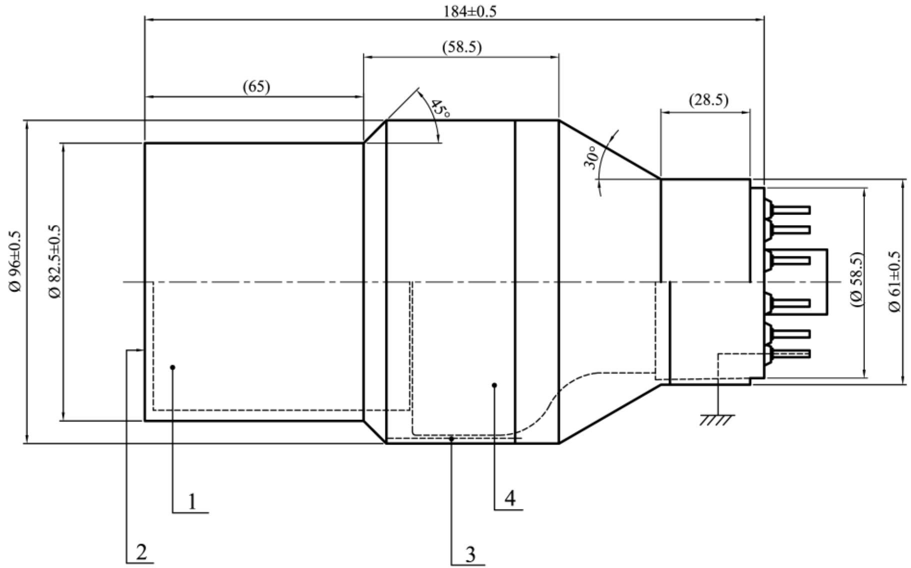

Drawing of ING-27: 1 – neutron generator target, 2 – α-detector (256pixel), 3 – signal connector of α-detector, 4 – high-voltage power connectors, 5 - low-voltage control connector

Drawing of $LaBr_3(Ce)$ γ-detector: 1 — the $LaBr_3(Ce)$ crystal, 2 — aluminum case of the detector, 3 — magnetic shielding, 4 — Hamamatsu R10233 PMT tube. Dimensions in the outline drawing are in mm.

Experimental setup

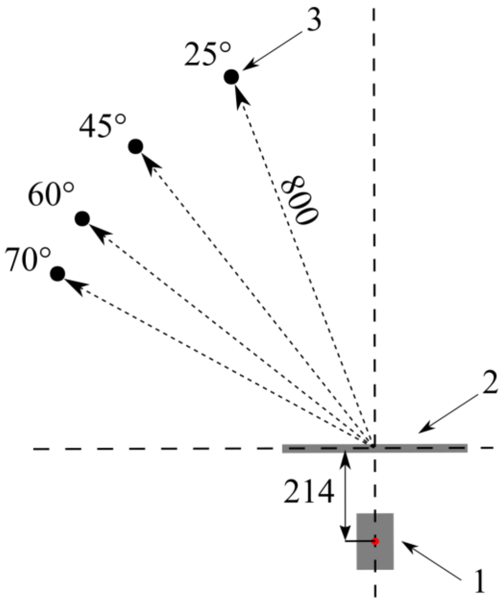

A setup for measuring cross sections and angular distributions of gamma rays in (n,n'x) reactions.

1- ING-27, 2 – Sample, 3 - $LaBr_3$(Ce) detectors. All dimensions are in mm.

Sample chracteristic

Sample	Density (g/cm^3)	Size (cm^3)	Isotopic composition
SiO_2	2.47	44 x 44 x 1.9	^{28}Si – 92.2%, ^{29}Si – 4.7%, ^{30}Si – 3.1% ^{16}O – 98.7%, ^{17}O – 0.04%, ^{18}O – 0.25%
Al	2.70	44 x 44 x 0.7	^{27}Al – 100%
Ti	4.34	44 x 44 x 0.9	^{46}Ti – 8.25%, ^{47}Ti – 7.44%, ^{48}Ti – 73.72%, ^{49}Ti – 5.41%, ^{50}Ti – 5.18%,
Fe	7.87	44 x 44 x 0.9	^{54}Fe – 5.84%, ^{56}Fe – 91.75%, ^{57}Fe – 2.11%, ^{58}Fe – 0.28

Measurement of "tagged" neutron beam profiles

2D-detector, made of 4 double-sided stripped position-sensitive Si-detectors

Each Si detector consists of 32 x 32 strips ~1.8 mm thick
Size of one detector: 60x60 mm^2
Total size: 120x120 mm^2
Thickness: 0.3 mm
Neutron detection efficiency: ~ 0.8%

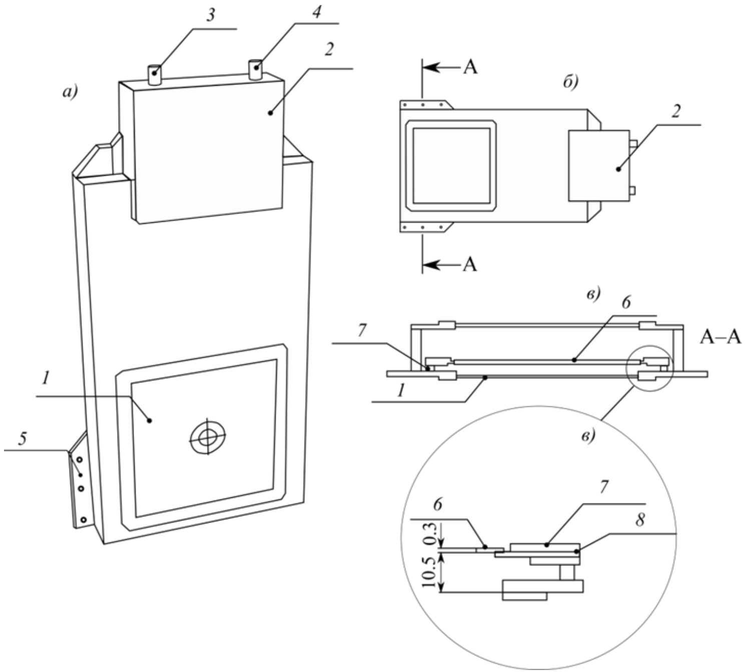

N. I. Zamytin et. al., Nucl. Instr. Meth. A898, 46 (2018)

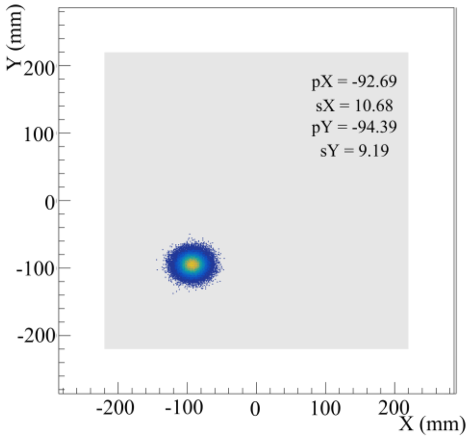

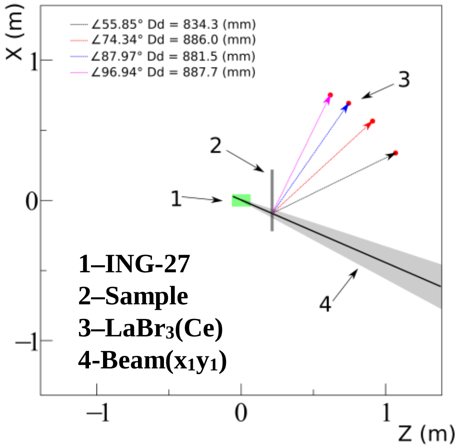

Data processing methodology. Time spectra

Examples of the time-of-flight spectra obtained.

Peaks are labelled with source reaction.

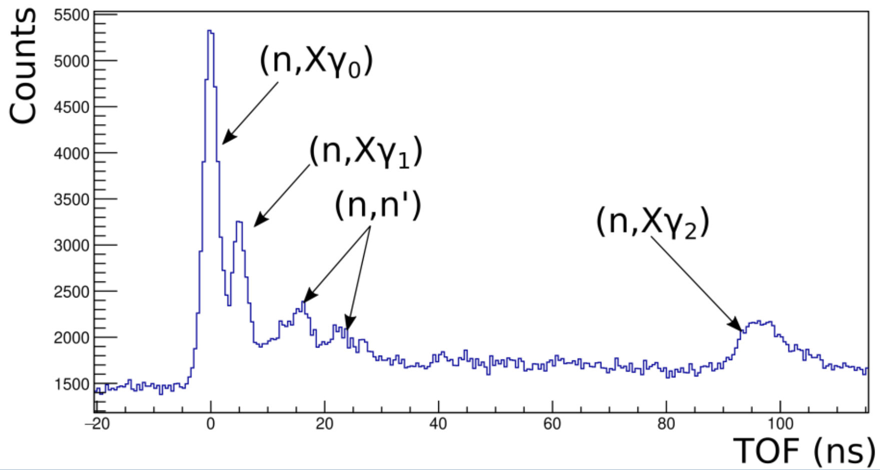

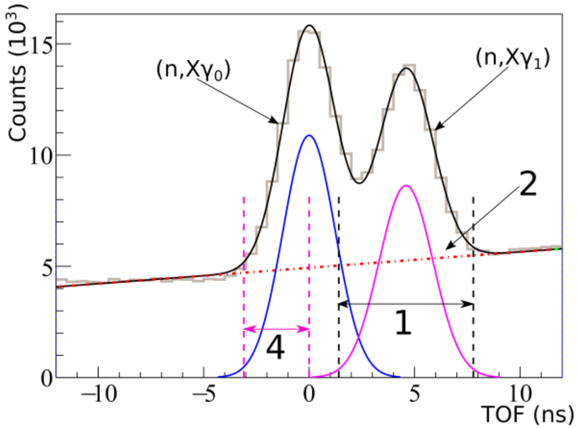

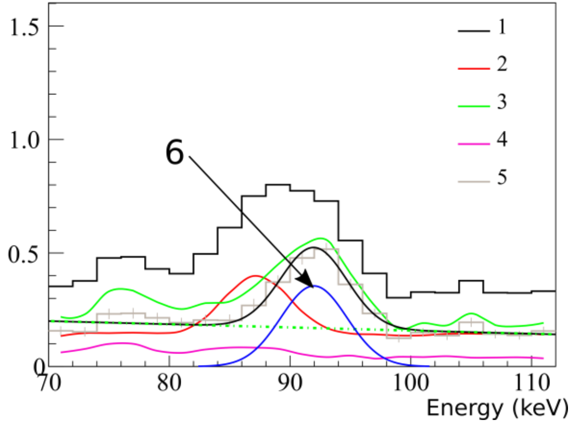

We identified two main sources of the background in our spectra.

a: Random coincidence (2). b: (n,Xγ$_0$) - γ from ING-27 (4)

Where: 1 – Full sample energy spectra, 3 – Sample–Random,

6 – Net spectra (without background from ING27).

And 6 is peak form sample 92 (keV) from $^{27}Al(n,\alpha)^{24}Na$.

Data processing methodology. Energy spectra

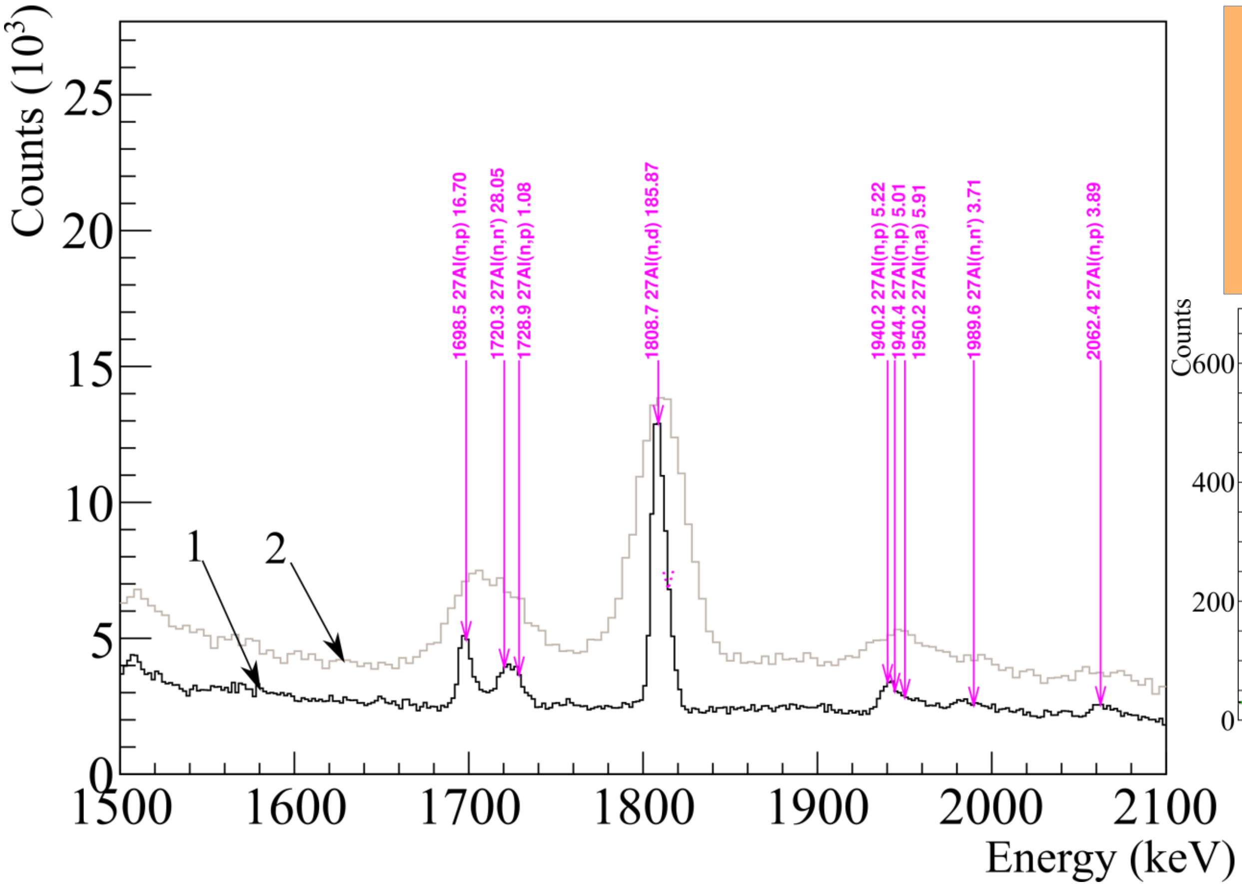

Where:

1 – HPGe detector,

2 – $LaBr_3$(Ce) detector.

The position of γ-peaks indetifecete by TalysLib.

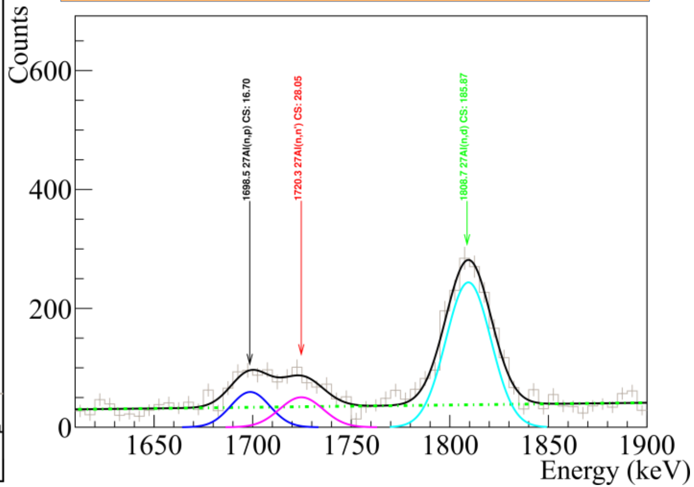

Data processing methodology. Calculation of cross sections

$$\frac{d\sigma}{d\Omega}(\theta) = \frac{N_p cos\xi}{4\pi N_\alpha n_{at} k} 10^{27} [\frac{mbarns}{sr}]$$

- Area of γ-peak — N_p
- Incident angle — ξ
- Number of tagged neutrons — N_α
- Surface density of atoms in the sample — n_{at}

Total reaction cross section:

$$\sigma = 2\pi \int_{-1}^{1} \frac{d\sigma}{d\Omega}(cos\theta)\ dcos\theta$$

$$k = \int_0^{x_0} \varepsilon(x) k_{ms}(x) k_{satt}(x) k_{iatt}(x) dx$$

- Sample thickness — x_0
- The total efficiency — $\varepsilon(x)$
- Multiple inelastic scattering — $k_{ms}(x)$
- Attenuation of γ-rays — $k_{satt}(x)$
- Attenuation of incident neutron — $k_{iatt}(x)$

- **The features of the experimental approach are the close geometry and the quite large sample**
- **All corrections changed significantly depending on the target thickness**
- **We could not consider the various correction independently**

Algorithm for determining the correction factor

There are two ways to calculate corrections:

- To calculate them independently in dependence on the sample thickness and take the integral
- **To simulate the total thickness-integrated correction in the GEANT4 using a separate ones as weighting factors**

Correction features:

- Multiple inelastic scattering overstates the number of emitted γ-rays
- Attenuation of incident neutrons and γ-rays understates the number of emitted γ-rays

Simulation features:

- 2 stage - neutron transport and γ-rays transport simulation
- The inelastic multiple scattering is used as a probability factor increasing the number of emitted γ-rays in comparison with its real number
- The inelastic multiple scattering correction calculates taking into account the energy dependence of emission cross section for specific γ-line taken from TALYS for each interaction point
- The correction factor resulted included thickness-integrated multiple scattering, absorption and efficiency coefficients

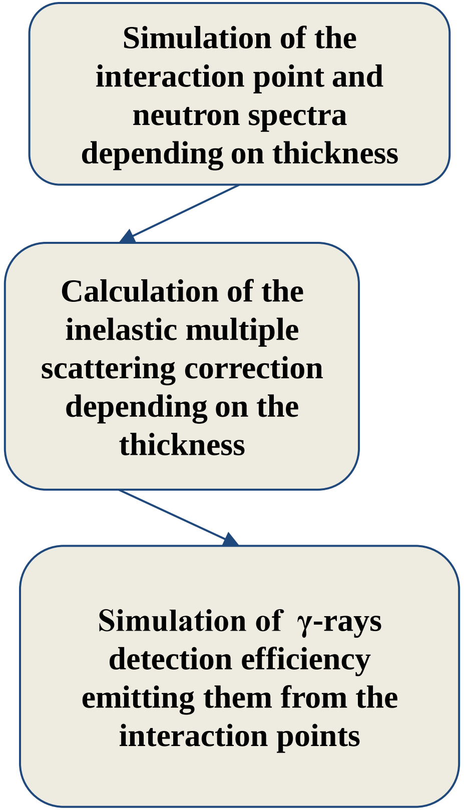

Example of the multiple scattering correction

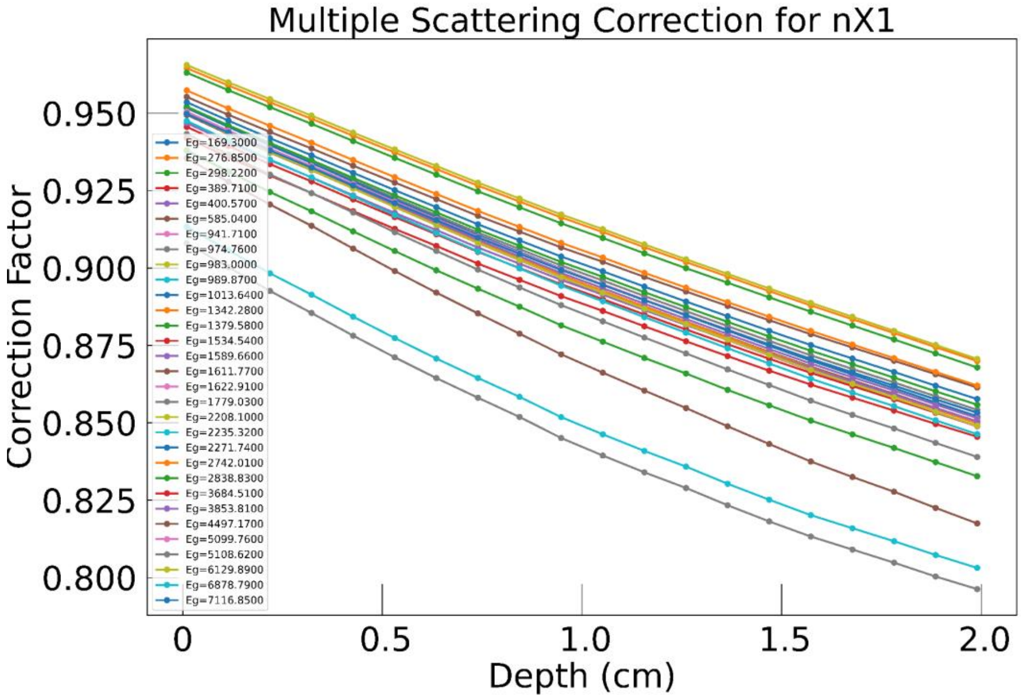

Multiple scattering correction factor depending on the sample thickness. The example corresponding to the SiO_2 sample and first vertical strip

Integrated correction factors using the example of the SiO_2 sample

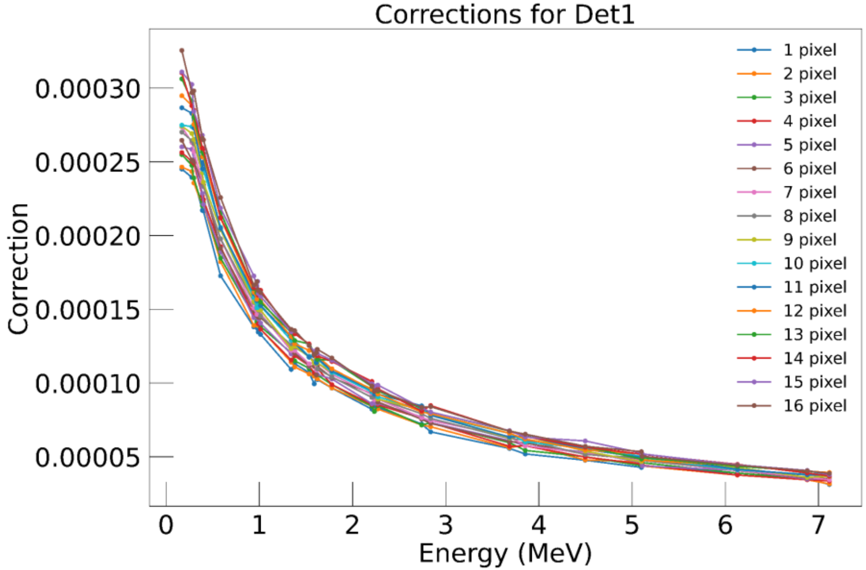

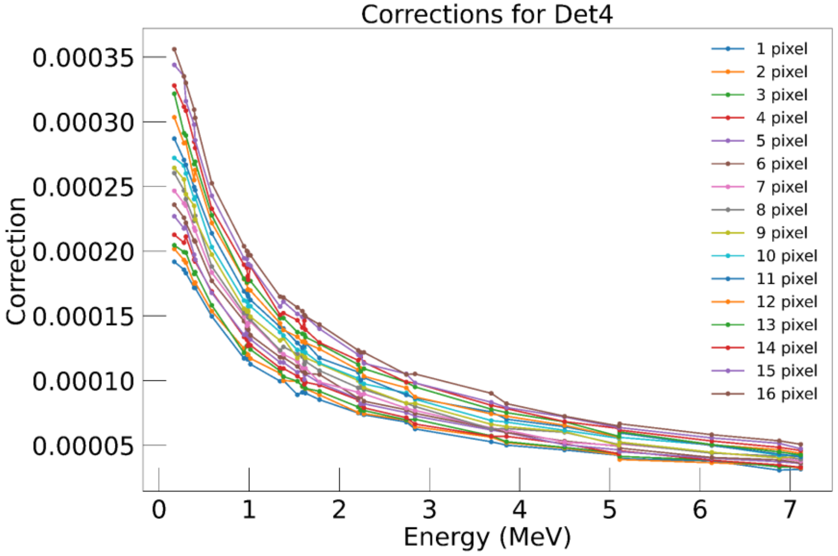

The correction factors including the attenuation correction, total efficiency and multiple inelastic scattering corresponding to the various $LaBr_3$ (Ce) detectors

Cross-section measurement results of oxygen

E_γ, keV	Reaction	σ_γ ($\Delta\sigma_\gamma$), mb/sr	Talys	Simakov
170	$^{16}O(n,p)^{16}N$	24±1	23	
298	$^{16}O(n,p)^{16}N$	17±1	23	
2742	$^{16}O(n,n')^{16}O$	27±1	50	38±4
3684	$^{16}O(n,\alpha)^{13}C$	41±1	72	58±5
3853	$^{16}O(n,n')^{16}O$	24±1	6	34±4
6129	$^{16}O(n,n')^{16}O$	100±2	131	148±10

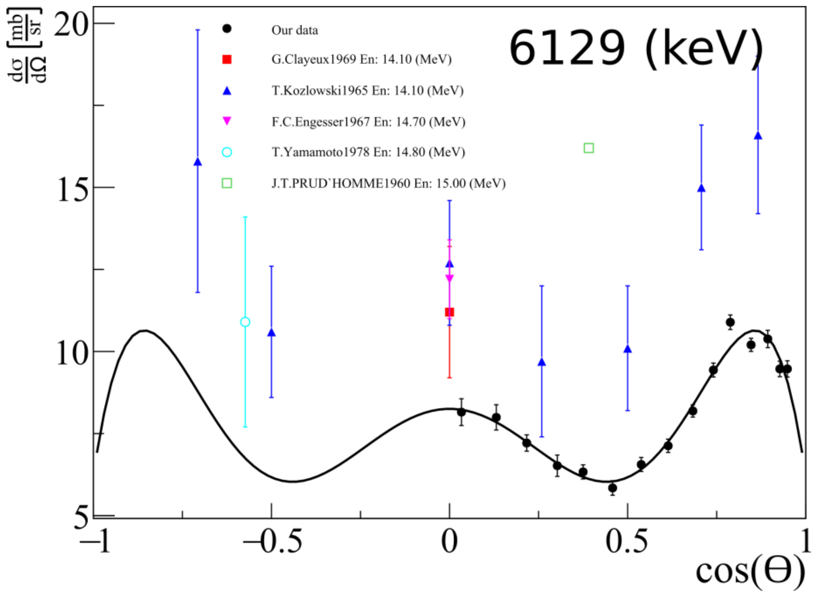

Ref.	α_2	α_4	α_6
Kozlowski1965 (152±4)	0.18 (0.09)	-0.27 (0.13)	-0.68 (0.13)
Grozdanov2024	0.36 (0.02)	0.08 (0.03)	-0.57 (0.03)
Our Data	**0.26 (0.03)**	**0.05 (0.04)**	**-0.52 (0.05)**

Cross-section measurement results of aluminium

E_γ, keV	Reaction	σ_γ ($\Delta\sigma_\gamma$), mb/sr	Talys	Simakov
90	$^{27}Al(n,\alpha)^{24}Na$	30±1	41	
792	$^{27}Al(n,n')^{27}Al$	26±1	11	
843	$^{27}Al(n,n')^{27}Al$	22±2	23	32±5
869	$^{27}Al(n,\alpha)^{24}Na$	14±1	14	
955	$^{27}Al(n,p)^{27}Mg$	11±2	15	
984	$^{27}Al(n,p)^{27}Mg$	27±1	28	28±4
1014	$^{27}Al(n,n')^{27}Al$	70±2	64	25±2
1129	$^{27}Al(n,d)^{26}Mg$	8±1	15	
1506	$^{27}Al(n,n')^{27}Al$	15±1	6	

E_γ, keV	Reaction	σ_γ ($\Delta\sigma_\gamma$), mb/sr	Talys	Simakov
1698	$^{27}Al(n,p)^{27}Mg$	29±2	17	30±3
1720	$^{27}Al(n,n')^{27}Al$	20±2	28	
1809	$^{27}Al(n,d)^{26}Mg$	132±1	186	184±10
2212	$^{27}Al(n,n')^{27}Al$	130±2	117	145±10
2298	$^{27}Al(n,n')^{27}Al$	28±2	18	
3004	$^{27}Al(n,n')^{27}Al$	100±2	83	111±6
3208	$^{27}Al(n,n')^{27}Al$	13±1	6	32±10

Cross-section measurement results of aluminium

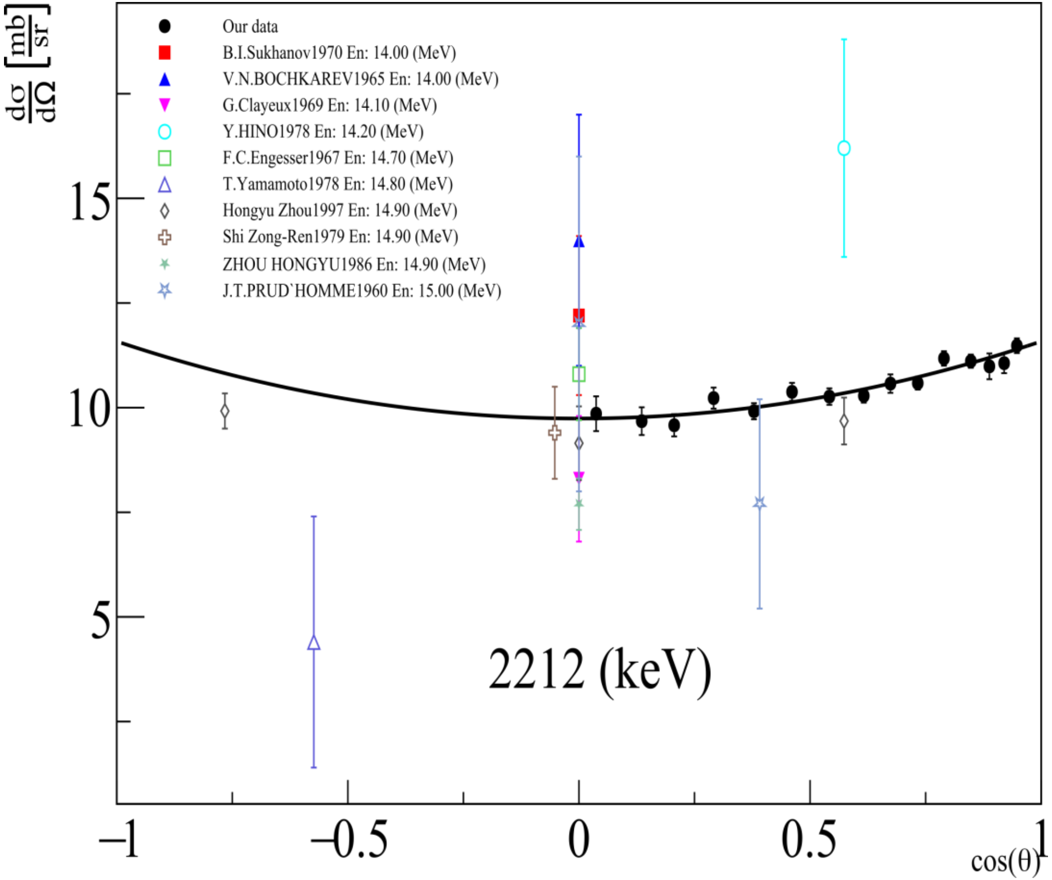

Ref.	a_2
Our Data	0.12±0.01
Zhou1997 (σ_γ = 121±1)	0.09±0.01

Cross-section measurement results of silicon

E_γ, keV	Reaction	σ_γ ($\Delta\sigma_\gamma$), mb/sr	Talys	Simakov
389	$^{28}Si(n,\alpha)^{25}Mg$	20±1	18	25±4
585	$^{28}Si(n,\alpha)^{25}Mg$	34±2	49	41±10
1379	$^{28}Si(n,\alpha)^{25}Mg$	35±2	8	32±5
1623	$^{28}Si(n,p)^{28}Al$	78±3	19	
1779	$^{28}Si(n,n')^{28}Si$	387±3	382	403±18
2217	$^{28}Si(n,p)^{28}Al$	39±2	23	28±4
2837	$^{28}Si(n,n')^{28}Si$	67±4	81	59±7
4497	$^{28}Si(n,n')^{28}Si$	26±2	20	

Cross-section measurement results of silicon

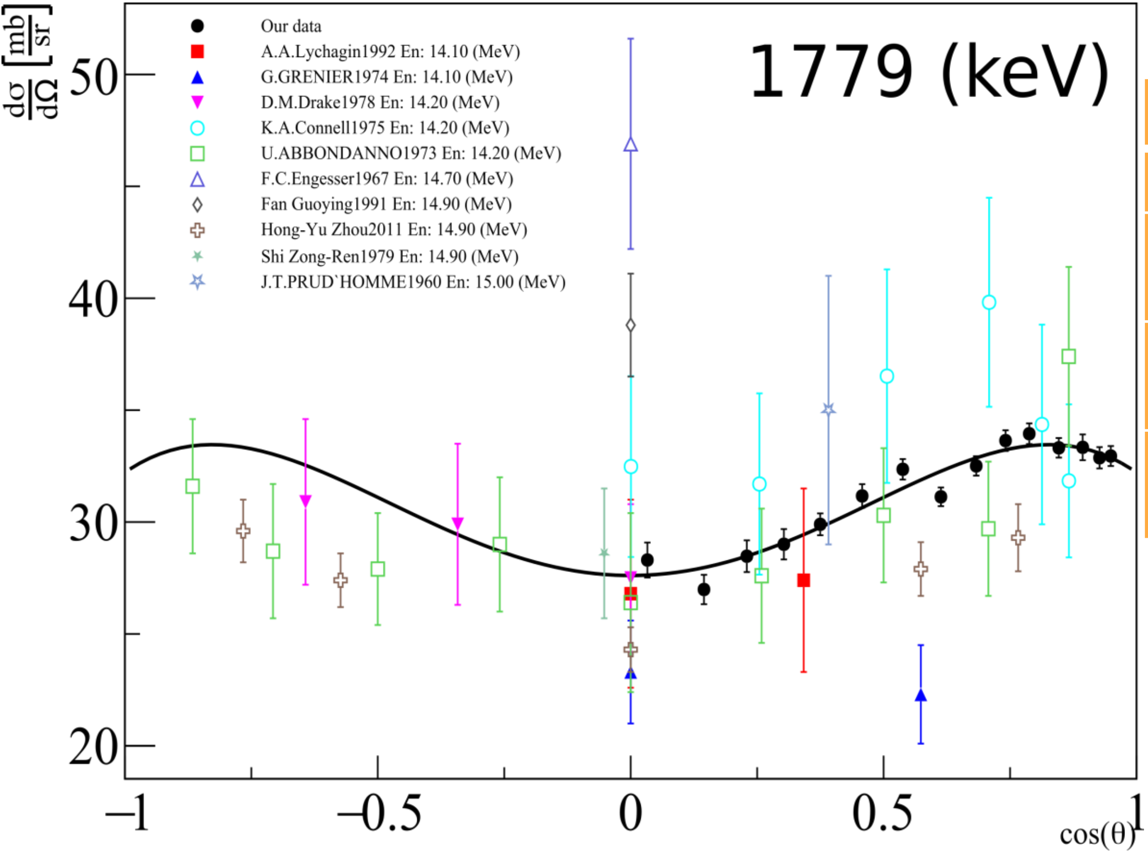

Ref.	α_2	α_4
Our Data	0.14±0.01	-0.09±0.02
U.ABBONDANNO 1973 (σ_γ = 940)	0.19±0.06	0.09±0.09
K.A. Connel1975 (σ_γ = 426)	-0.08±0.05	-0.33±0.10
Hong-Yu Zhou 2011 (σ_γ = 341)	0.18±0.02	-0.05±0.03

Cross-section measurement results of titanium

E_γ, keV	Reaction	σ_γ ($\Delta\sigma_\gamma$), mb/sr	Talys	Simakov
121	$^{48}Ti(n,p)^{48}Sc$	40±2	58	
130	$^{48}Ti(n,p)^{48}Sc$	50±2	69	
160	$^{48}Ti(n,2n)^{47}Ti$	197±2	143	404±40
175	$^{48}Ti(n,n')^{48}Ti$	45±2	18	
370	$^{48}Ti(n,p)^{48}Sc$	22±2	23	
889	$^{46}Ti(n,n')^{46}Ti$	55±2	58	62±7
944	$^{48}Ti(n,n')^{48}Ti$	51±2	28	47±6
983	$^{48}Ti(n,n')^{48}Ti$	691±3	478	666±61

E_γ, keV	Reaction	σ_γ ($\Delta\sigma_\gamma$), mb/sr	Talys	Simakov
1037	$^{48}Ti(n,n')^{48}Ti$	83±2	54	49±7
1120	$^{47}Ti(n,2n)^{46}Ti$	37±3	16	32±4
1312	$^{48}Ti(n,n')^{48}Ti$	330±4	209	238±27
1437	$^{48}Ti(n,n')^{48}Ti$	70±4	26	49±7
1542	$^{49}Ti(n,n')^{49}Ti$	29±2	9	32±4
2240	$^{48}Ti(n,n')^{48}Ti$	31±2	16	32±5
2375	$^{48}Ti(n,n')^{48}Ti$	80±2	30	57±9
2633	$^{48}Ti(n,n')^{48}Ti$	24±2	7	

Cross-section measurement results of titanium

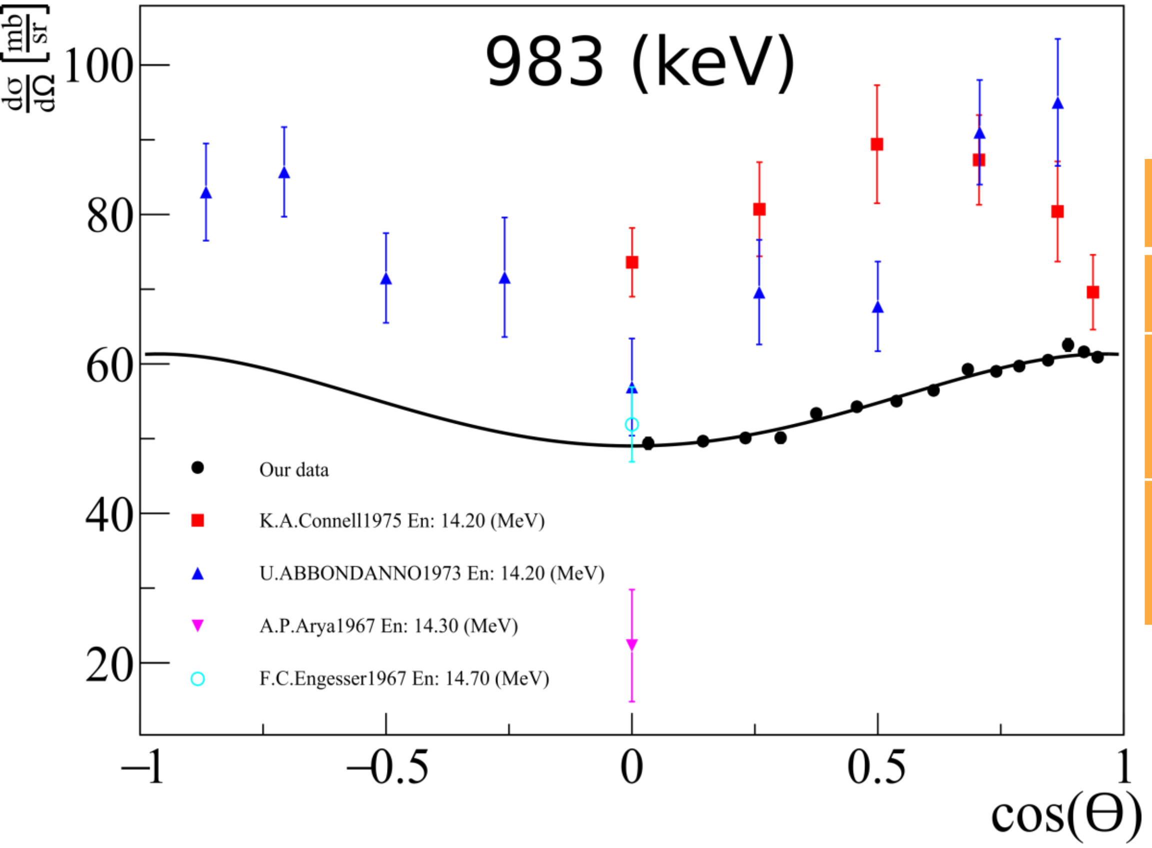

Ref.	α_2	α_4
Our Data	0.17±0.01	-0.06±0.01
U.ABBONDANNO 1973 (σ_γ = 940)	0.31±0.08	-0.11±0.12
K.A, Connel 1975 (σ_γ = 1019)	-0.03±0.02	-0.26±0.03

Cross-section measurement results of iron

E_γ, keV	Reaction	σ_γ ($\Delta\sigma_\gamma$), mb/sr	Talys	Simakov
125	$^{56}Fe(n,d)^{55}Mn$	41±2	25	
212	$^{56}Fe(n,p)^{56}Mn$	39±4	21	
314	$^{56}Fe(n,p)^{56}Mn$	6±2	6	
367	$^{56}Fe(n,n')^{56}Fe$	7±1	6	
377	$^{54}Fe(n,d)^{54}Mn$	5±2	9	
411	$^{56}Fe(n,2n)^{55}Fe$	22±1	50	53±7
477	$^{56}Fe(n,2n)^{55}Fe$	17±2	26	50±7
846	$^{56}Fe(n,n')^{56}Fe$	734±4	609	785±48
931	$^{56}Fe(n,2n)^{55}Fe$	78±2	132	126±25

E_γ, keV	Reaction	σ_γ ($\Delta\sigma_\gamma$), mb/sr	Talys	Simakov
1037	$^{56}Fe(n,n')^{56}Fe$	65±2	50	52±6
1238	$^{56}Fe(n,n')^{56}Fe$	331±4	293	238±27
1303	$^{56}Fe(n,n')^{56}Fe$	125±2	63	76±8
1670	$^{56}Fe(n,n')^{56}Fe$	40±2	28	36±6
1810	$^{56}Fe(n,n')^{56}Fe$	44±2	26	63±5
2598	$^{56}Fe(n,n')^{56}Fe$	31±2	16	35±5

Cross-section measurement results of iron

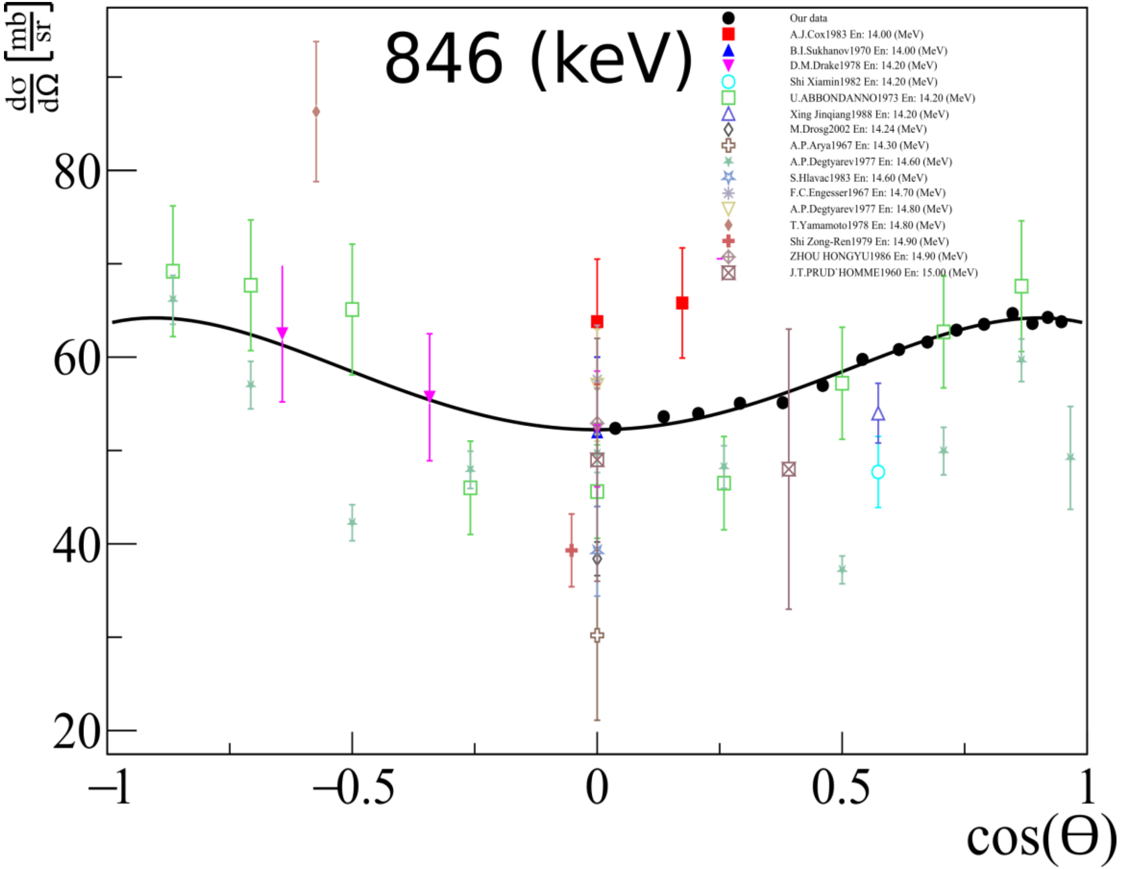

Ref.	α_2	α_4
Our Data	0.16±0.01	-0.07±0.01
U.ABBONDANNO 1973 (σ_γ = 716)	0.32±0.06	-0.20±0.09
A.P., Degtyarev 1977 (σ_γ = 627)	0.31±0.11	0.30±0.15

Conclusion

As a result of the experiment, the applicability of the discussed installation for measuring cross sections and angular distributions was demonstrated.

The data obtained demonstrate satisfactory agreement with the results of the most recent measurements performed by other authors.

For the first time, we measured the cross sections of 170, 280 keV lines from Oxygen. And from Aluminum 90, 792, 896, 955, 1129, 1506, 1720, 2298. And from Silicon 1623, 2217, 4497. And from Titanium 121, 130, 175, 370, 1037, 2633. Also from Iron 125, 212, 314, 367, 377.

Thanks for your attention!